RSC Advances

PAPER

View Article Online
View Journal | View Issue



Cite this: *RSC Adv.*, 2018, **8**, 38929

# A highly sensitive and selective fluorescent probe without quencher for detection of $Pb^{2+}$ ions based on aggregation-caused quenching phenomenon†

Qianyun Li,[ab] Yongmei Jia,[b] Zongcai Feng*[b] and Fang Liu*[a]

Received 23rd September 2018
Accepted 6th November 2018

DOI: 10.1039/c8ra07903j

rsc.li/rsc-advances

Lead is a highly toxic heavy metal, and various functional nucleic acid (FNA)-based biosensors have been developed for the detection of $Pb^{2+}$ in environmental monitoring. However, most fluorescence biosensors that have been reported were designed on the basis of a double-labeled (fluorophore and quencher group) DNA sequence, which not only involved an inconvenient organic synthesis but also restricted their wider use in practical applications. Here, we utilized a G-rich DNA sequence as a recognition probe and conjugated fluorene (CF) to develop a fluorescence sensor without a quencher based on the aggregation-caused quenching (ACQ) effect. In the presence of $Pb^{2+}$, the degree of aggregation of CF was reduced because $Pb^{2+}$ induced the formation of a G-quadruplex structure of the CF-DNA probe, and the fluorescence signal increased with the concentration of $Pb^{2+}$ (0–1 μM), with a limit of detection of 0.36 nM. This fluorescent probe without a quencher enables the sensitive and selective detection of $Pb^{2+}$. On the basis of these advantages, the CF-DNA probe represents a promising analytical method for detecting $Pb^{2+}$.

## 1. Introduction

$Pb^{2+}$ is a toxic heavy metal ion and has aroused widespread concern as it can cause severe impairments in the nervous system, kidney, and development of children even at low concentrations.[1–3] Owing to its bioaccumulation and highly toxic properties, it is urgently necessary to develop rapid and highly sensitive analytical methods for detecting $Pb^{2+}$ in environmental monitoring systems. Various instrumental techniques are widely used for the detection of $Pb^{2+}$ with high sensitivity and accuracy, including atomic absorption spectrometry (AAS),[4] inductively coupled plasma mass spectrometry (ICP-MS), and high-performance liquid chromatography (HPLC).[5,6] However, most of the abovementioned techniques are somewhat limited by the requirement for expensive and sophisticated equipment and a complicated sample pretreatment process. To overcome these limitations and disadvantages, a variety of novel sensors with high sensitivity and selectivity have been developed for detecting $Pb^{2+}$ in recent years. In contrast, fluorescence analytical methods possess the outstanding merits of high sensitivity, simplicity, and a fast response to targets and have received growing interest from researchers.[7,8] Many fluorescence biosensors have been designed for rapidly detecting targets on the basis of fluorogen–quencher pairs.[9,10] The fluorescence signal can be turned on or off by controlling the fluorogen and quencher. Thus far, researchers have achieved great progress in fluorescence sensors for the detection of metal ions by utilizing novel materials including organic fluorescent dyes,[11] gold nanoparticles,[6] metal–organic frameworks (MOFs),[12] and graphene oxide (GO).[13]

In the past decade, FNA-based biosensors have developed rapidly and shown great potential in the detection of heavy metal ions owing to their high specificity in binding to their target molecules, such as metal ions,[14,15] toxins, and enzymes.[16–19] Numerous fluorescence biosensors based on DNAs with specific sequences have been reported that can selectively react with metal ions to form stable metal-base pairs, for instance, G-rich DNA and thymine (T)-rich DNA.[20–22] For example, some groups have fabricated excellent DNA sensors based on DNAzymes (such as 8-17 DNAzyme and GR-5 DNAzyme), which have commonly been used for $Pb^{2+}$ sensors.[23,24] In the presence of $Pb^{2+}$, the catalytic activity of the DNAzyme was activated to cleave the substrate. Therefore, a new single-stranded DNA with a labelled fluorophore was produced, and the fluorescence signal changed. DNAzyme-based sensors enabled the detection of aqueous $Pb^{2+}$ with high sensitivity and high selectivity.[25,26]

$Pb^{2+}$ is able to selectively react with G-rich single-stranded DNA and induce the conformational change to a G-

[a]School of Materials Science and Engineering, South China University of Technology, Guangzhou 510640, Guangdong, China. E-mail: mcfliu@scut.edu.cn; fengzongcai921@163.com

[b]Institute for Advanced Materials, Lingnan Normal University, Zhanjiang 524048, Guangdong, China

† Electronic supplementary information (ESI) available. See DOI: 10.1039/c8ra07903j

quadruplex that consists of planar stacks of four guanines stabilized by Hoogsteen hydrogen bonding.[8,27] A thrombin-binding aptamer (G-rich DNA) labelled with a fluorophore and a quencher at the termini has been designed for the detection of $Pb^{2+}$ by exploiting the difference in the degree of fluorescence resonance energy transfer (FRET) upon binding to $Pb^{2+}$ ions.[28] In addition, a turn-on fluorescence sensor based on graphene oxide (GO) and a G-quadruplex for the detection of $Pb^{2+}$ has been developed on the basis of the significant difference in the binding capacity of GO with single-stranded DNA and the G-quadruplex.[29] According to the above detection methods, on the basis of the combination or separation of a fluorophore and a quencher group (such as GO, nanorod, or nanosheet) to achieve fluorescence quenching and recovery, sensitive and selective sensors have been constructed to detect targets using this strategy.[30,31] However, probes that contain both a fluorophore and a quencher group have the drawbacks of a complicated organic synthesis and difficulties in precisely controlling the distance between the fluorophore and the quencher group. Therefore, it is of great significance to develop a sensitive and simple unlabelled fluorescence sensor for detecting $Pb^{2+}$.

In this study, we utilized a G-rich DNA sequence as a recognition probe and conjugated fluorene (CF) to develop a fluorescence sensor without a quencher for detecting $Pb^{2+}$. In an aqueous solution, the hydrophobic fluorophore units of the probe (CFs) aggregated to form a core with a shell of hydrophilic DNA and caused the quenching of fluorescence owing to the ACQ phenomenon.[32] In the presence of $Pb^{2+}$, the CF-DNA probe bound to $Pb^{2+}$ and induced the conformational change to a G-quadruplex structure. The destruction of aggregates of CFs resulted in fluorescence enhancement. Furthermore, the fluorescent probe was employed in the detection of $Pb^{2+}$ and exhibited outstanding sensitivity and selectivity, which indicated its potential for applications in environmental monitoring.

# 2. Experimental

## 2.1 Materials and reagents

2,7-Dibromo-9,9-di-*n*-octylfluorene, ammonium acetate, *N*,*N*-dimethylformamide and *N*,*N*′-dicyclohexylcarbodiimide were purchased from Aladdin (Shanghai, China). Tetrakis(-triphenylphosphine)palladium(0) and 4-methoxycarbonylphenylboronic acid were purchased from J&K Scientific Co., Ltd (Beijing, China). $Pb(NO_3)_2$, $CaCl_2$, $Cd(NO_3)_2$, $Co(NO_3)_2$, $Fe(NO_3)_3$, $Mg(SO_4)_2$, $SbCl_3$, $AlCl_3$, $ZnSO_4$, $HgCl_2$, $KNO_3$, and $NaNO_3$ were purchased from Alfa Aesar Chemicals Co., Ltd (Shanghai, China) and Aladdin Bio-chem Technology Co., Ltd (Shanghai, China). All the other chemical reagents of analytical grade used in this study were purchased from Sinopharm (China) and were used without any further purification. Oligonucleotides with the sequence of 5′-$NH_2$-GGAAGGTGTGGAAGG-3′ were purchased from Sangon Biotech Co., Ltd (Shanghai, China) and were purified using high-performance liquid chromatography. The buffers used in this study were as follows: 10 mM Tris–HCl (120 mM NaCl, 5 mM KCl, pH = 7.4) and PBS buffer (10 mM, pH = 7.4). Ultrapure water was used throughout and was purified using a Milli-Q water system from Millipore (Billerica, MA, USA).

## 2.2 Apparatus

$^1$H NMR spectra were obtained with a Bruker Avance III spectrometer (400 MHz). The CF-DNA probe was purified by HPLC (Wufeng HPLC system, China). Fluorescence spectra and fluorescence intensity were determined using a Cary Eclipse F-4500 fluorescence spectrophotometer (Agilent Technologies, USA). UV-vis absorption spectra were recorded at room temperature with a UV-vis spectrophotometer (Shimadzu, Japan). Circular dichroism (CD) spectra were recorded with a circular dichroism spectrophotometer (Jasco, Japan). Dynamic light scattering (DLS) was measured with a nanoparticle size analyzer (90Plus Zeta, Brookhaven Instruments Corporation, USA). Both TLC and column chromatography apparatus were obtained from Qingdao Ocean Chemicals (Qingdao, China).

## 2.3 Synthesis of fluorescent probe without quencher

The synthetic route of the fluorophore is shown in Fig. S1† and was based on previous reports.[33,34] Details of the synthetic steps used for $CF_1$, $CF_2$ and $CF_3$ are described in the ESI.† $CF_3$ was dissolved in dry DMF (500 μL) and then added to the 5′-amino-modified $Pb^{2+}$-DNA probe (14 OD) in a total volume of 250 μL 0.1 μM sodium tetraborate buffer (pH = 8.5) and shaken overnight at 25 °C in a dark area. The product (CF-DNA probe) was purified by high-performance liquid chromatography (HPLC) with an Arcus sBP-C18 reversed-phase column. The UV-vis absorption of DNA (at 260 nm) was used to analyse the structure and determine the concentration. A 100 μM stock solution of the CF-DNA probe was prepared with ultrapure water for further use.

## 2.4 Fluorescence spectroscopy study for detection of $Pb^{2+}$

The excitation wavelength was set at 340 nm and the emission wavelength ranged from 350 nm to 600 nm with a slit width of 10.0 nm and a PMT voltage of 600 V. Fluorescence emission spectra were obtained by recording the emission from 350 nm to 600 nm with a 50 μL quartz cuvette containing a 50 μL solution. A series of diluted CF-DNA solutions of different concentrations were added to PBS buffer to a total of 70 μL. After incubation for a period of time at 30 °C, the fluorescence intensity was recorded in a 50 μL cuvette. An aqueous solution of CF-DNA containing a 1 μM $Pb^{2+}$ solution was added and incubated for 5, 10, 15, 30, and 45 min with shaking at 500 rpm at 30 °C to choose a suitable reaction time. To optimize the reaction temperature, a 10 μM $Pb^{2+}$ solution was added in a reaction buffer containing 100 nM CF-DNA probe and shaken at 4, 15, 25, 30 and 37 °C. The CF-DNA probe with various concentrations (0–500 μM) of $Pb^{2+}$ ions in PBS buffer was incubated under the optimized conditions.

## 2.5 Specificity analysis

An assay for selectivity for $Pb^{2+}$ was conducted according to the same procedure as for $Pb^{2+}$ except that $Pb^{2+}$ was replaced with $Mg^{2+}$, $Ca^{2+}$, $Zn^{2+}$, $Co^{2+}$, $Sb^{3+}$, $Al^{3+}$, $Hg^{2+}$, $Na^+$, and $K^+$.

 

### 2.6 Analysis of $Pb^{2+}$ in real samples

Two different environmental samples, namely, samples of ocean water and lake water, were used in this study. The reliability of the method in practical applications was tested by determining the recovery rate for actual water samples. The two real water samples were taken from Ruiyun Lake and the South China Sea in Zhanjiang City, Guangdong Province, China, respectively. Suspensions and solid impurities were removed by membrane filtration after centrifugation at 10 000 rpm for 5 min. The samples were spiked with different concentrations of standard samples of $Pb^{2+}$. All procedures were identical to those mentioned above.

## 3. Results and discussion

### 3.1 Design of the fluorescence sensing platform based on the ACQ effect

In this assay, the nucleic acid probe was designed on the basis of the aggregation-caused quenching (ACQ) phenomenon with only a fluorophore but no quencher. The sensing mechanism of the method is shown in Scheme 1. Firstly, the signal reporter CF is a fluorescent core with ACQ characteristics.[34,35] The 5′-end of the $Pb^{2+}$-DNA probe was modified with an amino group to react with the CF active ester, and the CF-DNA probe was synthesized. Therefore, the hydrophobic fluorophore unit (conjugated fluorene) was linked to the hydrophilic $Pb^{2+}$-DNA probe *via* an amide bond. The CF-DNA probe can form micelles in an aqueous solution owing to the hydrophobic CF core and hydrophilic DNA shell. The aggregation of the CFs caused the quenching of fluorescence, and relatively low fluorescence intensity was exhibited in the absence of $Pb^{2+}$.[36,37] Upon the addition of $Pb^{2+}$, $Pb^{2+}$ bound to CF-DNA specifically induced the conformational change to the G-quadruplex structure.

Such conformational changes promoted the steric hindrance effect between CF-DNA probe molecules and led to enhanced dispersion of the CF hydrophobic units. The diameter of CF-DNA micelles markedly decreased according to the results of DLS (Fig. S5†). Therefore, the ACQ effect of the CF-DNA probe weakened in the presence of $Pb^{2+}$. The fluorescence intensity increased in the detection system.

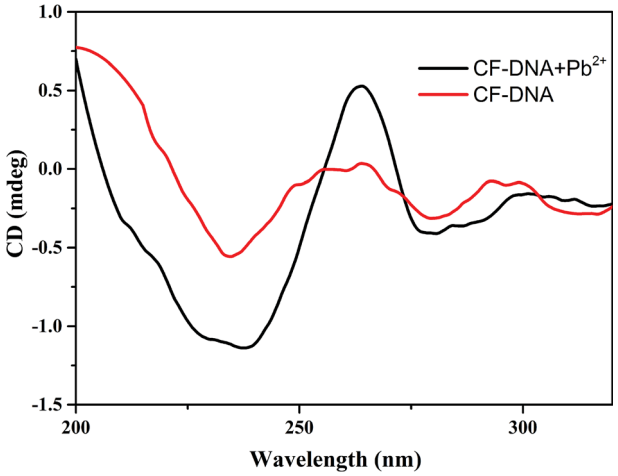


Fig. 1 Circular dichroism spectra of CF-DNA (5 μM) in the absence and presence of $Pb^{2+}$ (5 μM).

To confirm the conformational changes in the CF-DNA probe in the presence of $Pb^{2+}$, circular dichroism (CD) spectra were recorded in our study. As shown in Fig. 1, 5 μM $Pb^{2+}$ in PBS buffer induced 2 μM CF-DNA to undergo a structural change from a random coil to a G-quadruplex. Upon the addition of 5 μM $Pb^{2+}$ to the CF-DNA probe, we observed enhancements in the positive peak around 260 nm and the negative peak around 240 nm, which suggested the formation of the G-quadruplex. It has been reported that the CD spectrum of a "parallel" G-quadruplex has a positive peak around 260 nm and a negative peak around 240 nm.[38,39] The changes in the CD spectrum upon binding to $Pb^{2+}$ suggested the coexistence of the G-quadruplex.

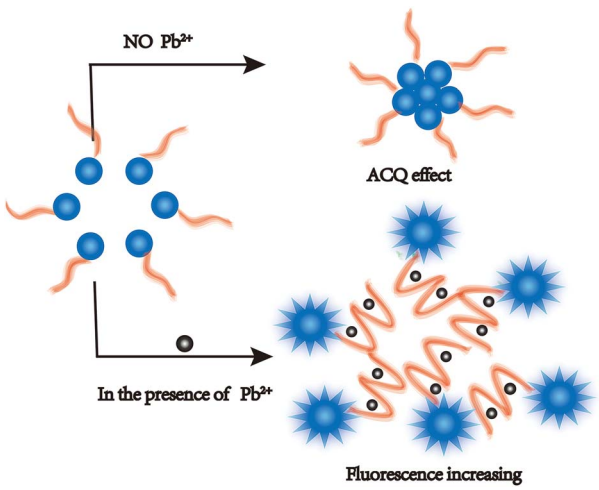


Scheme 1 Schematic illustration of analytical method for detecting $Pb^{2+}$ by utilizing the CF-DNA probe.

### 3.2 Synthesis, purification and identification of CF-DNA probe

CFs were synthesized according to a previous report,[34,35] modified with an active ester and then reacted with the $NH_2$-modified DNA probe. The fluorophore was successfully conjugated to the oligonucleotide *via* an amide bond.[40] To determine whether the $Pb^{2+}$-DNA probe was successfully linked to the CF derivative, the purification and structural analysis of the CF-DNA probe were conducted by HPLC and UV-vis absorption spectroscopy. The results of the purification of the CF-DNA probe by HPLC are shown in Fig. S6.† The retention time of the $Pb^{2+}$-DNA probe was 16.5 min, whereas the retention time of the CF-DNA probe was 18.6 min under the same purification conditions. The UV-vis absorption spectrum of the CF-DNA probe is shown in Fig. 2. The UV-vis absorption peaks of the $Pb^{2+}$-DNA probe (at 260 nm) and CF (at 340 nm) were used to analyse the structure.

The UV-vis absorption spectra displayed the two peaks at 260 nm and 340 nm of the CF-DNA probe,[41] which indicated the successful conjugation of CFs to the $Pb^{2+}$-DNA probe.

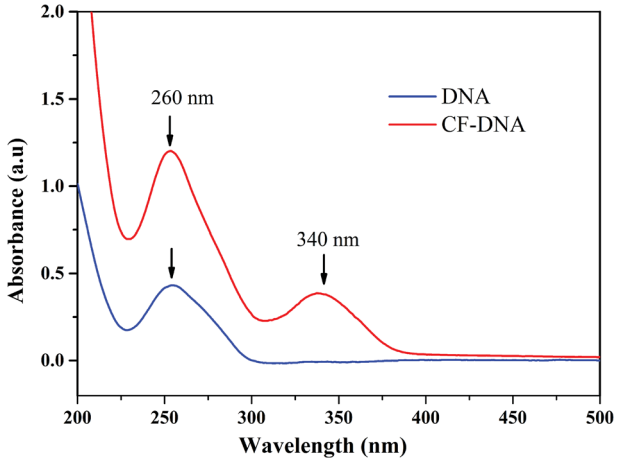


Fig. 2 UV-vis spectroscopic analysis of CF-DNA probe.

### 3.3 Detection of $Pb^{2+}$

In order to achieve high sensitivity and selectivity in the detection of $Pb^{2+}$, the concentration of CF-DNA, incubation time, temperature and buffer were investigated. To investigate the influence of the buffer composition, the CF-DNA probe and $Pb^{2+}$ were tested in two different buffer systems, namely, PBS buffer (pH 7.4) and Tris–HCl buffer (pH 7.0), respectively. The fluorescence phenomenon of the CF-DNA probe was better in PBS buffer than in Tris–HCl buffer. Upon the addition of $Pb^{2+}$, we obtained a better signal response for the detection of $Pb^{2+}$ in PBS buffer than in Tris–HCl buffer (Fig. S7†). Hence, PBS buffer was selected for the following analysis.

The concentration of the CF-DNA probe played an important role in binding to $Pb^{2+}$ ions and the performance of the biosensor. Firstly, the change in the fluorescence of the CF-DNA probe upon an increase in concentration was studied. The fluorescence intensity of the system increased as the concentration of CF-DNA increased from 1 nM to 500 nM (Fig. S8†). To obtain a good fluorescence phenomenon for the subsequent detection of $Pb^{2+}$, a concentration of CF-DNA of 100 nM was selected for the subsequent experiments. Several experiments were conducted to determine the optimal incubation time and temperature. The results for the optimal incubation time are shown in Fig. S9(A).† With an increase in the incubation time, the fluorescence intensity of the system increased gradually up to 45 min. During the early incubation period, the fluorescence intensity increased rapidly and tended to reach a plateau as the time increased to 15 min, which implied that most of the $Pb^{2+}$ ions interacted with the CF-DNA probe. As shown in Fig. S9(B),† good fluorescence performance for detection was achieved when $Pb^{2+}$ interacted with the CF-DNA probe below 30 °C. Hence, 30 °C was selected as the optimal temperature for the subsequent experiments.

### 3.4 Sensitivity and selectivity of the CF-DNA probe

To assess the sensitivity of the detection of $Pb^{2+}$, a series of concentrations of $Pb^{2+}$ were added to the solution of the CF-DNA probe, and the fluorescence emission spectra were recorded. The CF-DNA probe exhibited a certain fluorescence intensity at 415 nm in the absence of $Pb^{2+}$ (Fig. S10†). Many hydrophobic fluorophores of the CF-DNA probe aggregated and caused the ACQ phenomenon. Fig. 3(A) shows the fluorescence spectra of the CF-DNA probe after incubation with different concentrations of $Pb^{2+}$.

As observed in Fig. 3(A), the fluorescence signal gradually increased when the concentration of $Pb^{2+}$ increased from 0 to 1 μM, which implied that the increasing concentration of $Pb^{2+}$ induced the CF-DNA probe to form a G-quadruplex structure. The fluorophore units dispersed and the degree of aggregation decreased, so that the fluorescence signal increased markedly. The fluorescence intensity of the CF-DNA probe at 415 nm was enhanced upon the increase in the $Pb^{2+}$ concentration. This result was in accordance with the fact that a higher concentration of $Pb^{2+}$ can lead to the formation of $Pb^{2+}$ G-quadruplex structures, which accordingly results in the dispersion of hydrophobic CF moieties and the emission of stronger fluorescence. The spectra demonstrate that the increase in

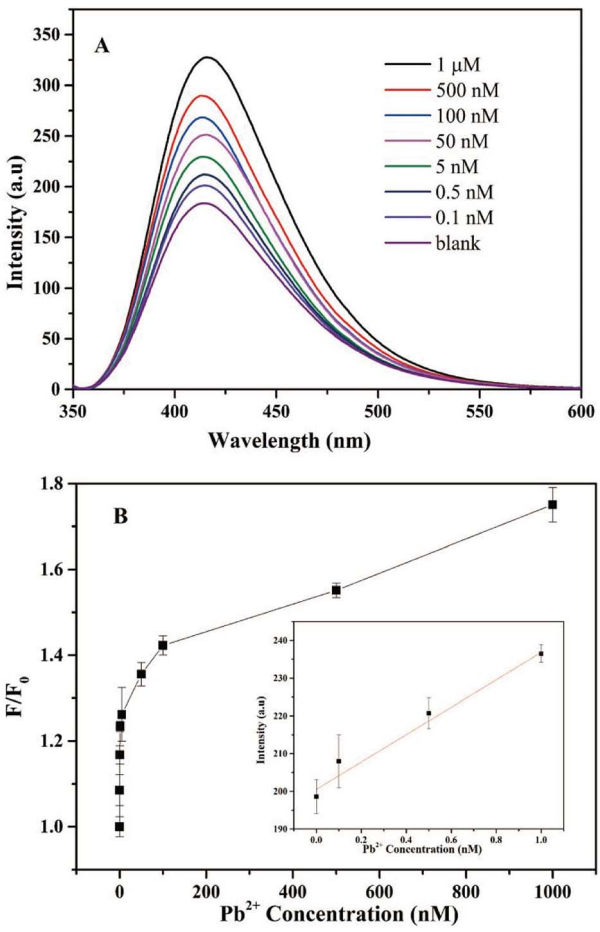


Fig. 3 (A) Fluorescence response of CF-DNA probe at different concentrations of $Pb^{2+}$ based on the ACQ effect. (B) Plot of fluorescence enhancement ($F/F_0$) at 415 nm as a function of the $Pb^{2+}$ concentration. $F$ is the fluorescence intensity of the CF-DNA probe with different concentrations of $Pb^{2+}$, and $F_0$ is the fluorescence intensity of the CF-DNA probe. The inset shows the change in fluorescence intensity with the $Pb^{2+}$ concentration over the range from 0 to 1 nM.

Table 1 Detection of $Pb^{2+}$ in real water samples using the proposed $Pb^{2+}$ fluorescent probe[a]

| Sample | | $Pb^{2+}$ spiked (nM) | $Pb^{2+}$ recovered mean[a] ± SD[b] | Recovery (%) |
|---|---|---|---|---|
| South China Sea | 1 | 0 | n | — |
| | 2 | 0.5 | $0.503^{a} \pm 0.02^{b}$ | 101 |
| | 3 | 1 | $0.988^{a} \pm 0.015^{b}$ | 98.8 |
| Ruiyun Lake | 1 | 0 | n | — |
| | 2 | 0.5 | $0.483^{a} \pm 0.03^{b}$ | 96.6 |
| | 3 | 1 | $1.06^{a} \pm 0.03^{b}$ | 106 |

[a] n: no $Pb^{2+}$ was detected.

fluorescence intensity at 415 nm was positively correlated with the concentration of $Pb^{2+}$. The curve in the inset of Fig. 3(B) represents the linear response of the CF-DNA probe to the $Pb^{2+}$ concentration over the range from 0 to 1 nM ($R^2 = 0.98$). The limit of detection (LOD) was calculated to be 0.36 nM on the basis of $3\sigma/S$ (where $\sigma$ is the standard deviation of the blank solution, and $S$ is the slope of the calibration curve). For comparison, the linear ranges and detection limits for the detection of $Pb^{2+}$ by different sensors are listed in Table S1.† In comparison with related methods, the advantages of this method are its simplicity, quick response, and high sensitivity and selectivity for the detection of $Pb^{2+}$.[37,38,42,43] As a result, the LOD of the CF-DNA probe was superior in comparison with those of previously reported $Pb^{2+}$ sensors.

In order to investigate the specificity and selectivity of the CF-DNA probe, some common metal ions with different valences (*e.g.*, $Cu^{2+}$, $Mg^{2+}$, $Ca^{2+}$, $Co^{2+}$, $Sb^{3+}$, $Zn^{2+}$, $Al^{3+}$, $Hg^{2+}$, $Na^{+}$, and $K^{+}$) were selected to conduct control experiments. As shown in Fig. 4, the other metal ions exhibited relatively lower fluorescence intensity in comparison with $Pb^{2+}$ under the same conditions. Only $Pb^{2+}$ led to an obvious increase in the fluorescence intensity of the system under the same conditions. This superior specificity is attributed to the property whereby $Pb^{2+}$ can specifically induce the formation of a G-quadruplex.

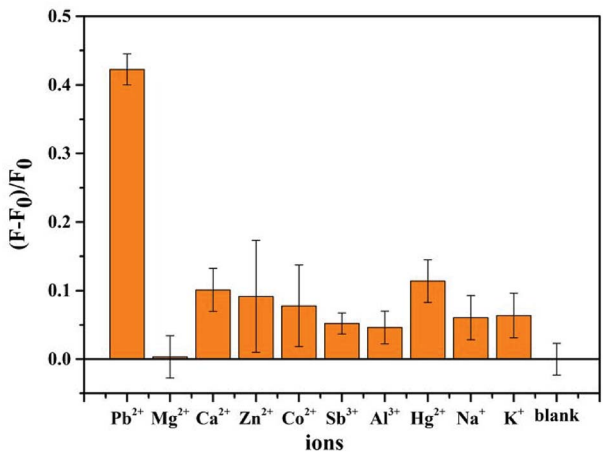


Fig. 4 Selectivity of 100 nM CF-DNA probe for the detection of $Pb^{2+}$ over other common ions. Relative fluorescence intensity of CF-DNA probe in the presence of 0.1 μM $Pb^{2+}$ and 1 μM other common metal ions. $F_0$ and $F$ are the maximum fluorescence intensities of the CF-DNA probe before and after the addition of metal ions.

Therefore, the selectivity assay demonstrated the remarkable selectivity of the CF-DNA probe for $Pb^{2+}$ when the other similar metal ions were present at higher concentrations.

The reproducibility of the proposed method was also investigated by performing five repeated experiments for the detection of 1 nM, 5 nM, and 100 nM $Pb^{2+}$ under the same conditions. The relative standard deviation (RSD) of the proposed sensor was found to be 3.7%, 4.2% and 4.5%, respectively. The stability of the CF-DNA probe was assessed by storing the prepared probe at 4 °C for at least one week. The results indicated that this probe retained 95% of its initial response after a storage period of 10 days (Fig. S11†). These results revealed that the reproducibility and stability of this probe were acceptable.

### 3.5 Detection of $Pb^{2+}$ in real samples

To assess the feasibility and application potential of this approach, different environmental water samples were collected from the South China Sea and Ruiyun Lake in Zhanjiang. The water samples were filtered through a filter membrane to remove any impurities. All the water samples were spiked with a $Pb^{2+}$ solution of a standard concentration and analysed by triplicate tests. The results are summarized in Table 1. According to the recovery analysis, the recoveries were in the range of 96.6–106%. These results demonstrated the practicality of using our CF-DNA probe for the detection of $Pb^{2+}$ ions in environmental samples.

## 4. Conclusions

For the purpose of detecting $Pb^{2+}$, a simplified, fast, highly selective and highly sensitive biosensor was developed in this study. The CF-DNA probe consisted of two components. CFs were employed as a signal reporter on the basis of the ACQ effect. The other component was a G-rich DNA probe, which is widely utilized as a classical recognition element and was employed as a reporter. This fluorescent probe for detecting $Pb^{2+}$ avoids a difficult synthesis and labelling with a quencher by utilizing the inherent ACQ effect. In comparison with previous methods for the analysis of $Pb^{2+}$, the fluorescent probe that was designed exhibited high sensitivity with an LOD of 0.36 nM. This sensor also provides excellent selectivity for $Pb^{2+}$ in relation to other potentially coexisting metal ions. In addition, assays of real water samples exhibited satisfactory results

and demonstrated application potential for detecting $Pb^{2+}$ in actual environmental samples.[44]

## Conflicts of interest

There are no conflicts to declare.

## Acknowledgements

We gratefully acknowledge the support of the National Natural Science Foundation of China (21705071), the Natural Science Foundation of Guangdong Province of China (2016A030310362), the Initiatory Financial Support from Lingnan Normal University (ZL1611) and the Resource and Chemical Engineering Technology Research Center of Western Guangdong Province.

## Notes and references

1 Q. J. Calvo, F. Arduini, A. Amine, V. K. Van, G. Palleschi and D. Moscone, *Anal. Chim. Acta*, 2012, **736**, 92–99.
2 S. Dolati, M. Ramezani, K. Abnous and S. M. Taghdisi, *Sens. Actuators, B*, 2017, **246**, 864–878.
3 Q. He, E. W. Miller, A. P. Wong and C. J. Chang, *J. Am. Chem. Soc.*, 2006, **128**, 9316–9317.
4 A. Sixto, M. Fiedorukpogrebniak, M. Rosende, D. Cocovisolberg, M. Knochen and M. Miró, *J. Anal. At. Spectrom.*, 2016, **31**, 473–481.
5 F. Arduini, J. Q. Calvo, G. Palleschi, D. Moscone and A. Amine, *Trends Anal. Chem.*, 2010, **29**, 1295–1304.
6 C. Zhang, C. Lai, G. Zeng, D. Huang, L. Tang, C. Yang, Y. Zhou, L. Qin and M. Cheng, *Biosens. Bioelectron.*, 2016, **81**, 61–67.
7 C. Wang, H. Cheng, Y. Huang, Z. Xu, H. Lin and C. Zhang, *Analyst*, 2015, **140**, 5634–5639.
8 C. Wang, H. Cheng, Y. Sun, Z. Xu, H. Lin, Q. Lin and C. Zhang, *Microchim. Acta*, 2015, **182**, 695–701.
9 Y. Zhu, Y. Cai, L. Xu, L. Zheng, L. Wang, B. Qi and C. Xu, *ACS Appl. Mater. Interfaces*, 2015, **7**, 7492–7496.
10 L. Guo, Y. Hu, Z. Zhang and Y. Tang, *Anal. Bioanal. Chem.*, 2018, **410**, 287–295.
11 D. X. Xie, Z. J. Ran, Z. Jin, X. B. Zhang and D. L. An, *Dyes Pigm.*, 2013, **96**, 495–499.
12 Y. Yu, Y. Chao, Y. Niu, J. Chen, Y. Zhao, Y. Zhang, R. Gao and J. He, *Biosens. Bioelectron.*, 2017, **101**, 297.
13 Y. Feng, X. Shao, K. Huang, J. Tian, X. Mei, Y. Luo and W. Xu, *Chem. Commun.*, 2018, **54**, 8036–8039.
14 J. Liu, A. K. Brown, X. Meng, D. M. Cropek, J. D. Istok, D. B. Watson and Y. Lu, *Proc. Natl. Acad. Sci. U. S. A.*, 2007, **104**, 2056–2061.
15 M. Rajendran and A. D. Ellington, *Anal. Bioanal. Chem.*, 2008, **390**, 1067–1075.
16 D. Li, W. Cheng, Y. Yan, Y. Zhang, Y. Yin, H. Ju and S. Ding, *Talanta*, 2016, **146**, 470.
17 M. Mohammadniaei, T. Lee, J. Yoon, D. Lee and J. W. Choi, *Biosens. Bioelectron.*, 2017, **98**, 292–298.
18 W. Chen, Y. Chen, M. Wang and Y. Chi, *Analyst*, 2018, **143**, 1575–1582.
19 S. Liu, W. Wei, Y. Wang, L. Fang, L. Wang and F. Li, *Biosens. Bioelectron.*, 2016, **80**, 208–214.
20 P. J. Huang, B. C. Van and J. Liu, *Analyst*, 2016, **141**, 3788.
21 Y. Miyake, H. Togashi, M. Tashiro, H. Yamaguchi, S. Oda, M. Kudo, Y. Tanaka, Y. Kondo, R. Sawa and T. Fujimoto, *J. Am. Chem. Soc.*, 2006, **128**, 2172–2173.
22 Y. Wu, S. Zhan, L. Xu, W. Shi, T. Xi, X. Zhan and P. Zhou, *Chem. Commun.*, 2011, **47**, 6027–6029.
23 D. Nie, H. Wu, Q. Zheng, L. Guo, P. Ye, Y. Hao, Y. Li, F. Fu and Y. Guo, *Chem. Commun.*, 2012, **48**, 1150.
24 X. Zhu, Z. Lin, L. Chen, B. Qiu and G. Chen, *Chem. Commun.*, 2009, **40**, 6050–6052.
25 Q. Zhang, Y. Cai, H. Li, D. M. Kong and H. X. Shen, *Biosens. Bioelectron.*, 2012, **38**, 331–336.
26 H. Li, Q. Zhang, Y. Cai, D. M. Kong and H. X. Shen, *Biosens. Bioelectron.*, 2012, **34**, 159–164.
27 H. Xu, P. Xu, S. Gao, S. Zhang, X. Zhao, C. Fan and X. Zuo, *Biosens. Bioelectron.*, 2013, **47**, 520–523.
28 C. W. Liu, C. C. Huang and H. T. Chang, *Anal. Chem.*, 2009, **81**, 2383–2387.
29 X. Li, G. Wang, X. Ding, Y. Chen, Y. Gou and Y. Lu, *Phys. Chem. Chem. Phys.*, 2013, **15**, 12800–12804.
30 J. Chen, Y. Wang, W. Li, H. Zhou, Y. Li, C. Yu and A. Chem, *Anal. Chem.*, 2014, **86**, 9866–9872.
31 Z. Qing, X. He, T. Qing, K. Wang, H. Shi, D. He, Z. Zou, L. Yan, F. Xu and X. Ye, *Anal. Chem.*, 2013, **85**, 12138–12143.
32 B. Liu, S. Wang, G. C. Bazan and A. Mikhailovsky, *J. Am. Chem. Soc.*, 2003, **125**, 13306–13307.
33 R. R. Nayak, O. K. Nag, Y. W. Han, S. Hwang, D. Vak, D. Korystov, Y. Jin and H. Suh, *Curr. Appl. Phys.*, 2009, **9**, 636–642.
34 E. Ergen, M. Weber, J. J. Dr, A. H. Dr and K. M. Dr, *Chemistry*, 2006, **12**, 3707.
35 Y. Jia, P. Gao, Y. Zhuang, M. Miao, X. Lou and F. Xia, *Anal. Chem.*, 2016, **88**, 6621.
36 T. Li, S. Dong and E. Wang, *J. Am. Chem. Soc.*, 2010, **132**, 13156–13157.
37 S. Dasgupta, S. A. Shelke, N. S. Li and J. A. Piccirilli, *Chem. Commun.*, 2015, **51**, 9034–9037.
38 T. Li, S. Dong and E. Wang, *J. Am. Chem. Soc.*, 2010, **132**, 13156.
39 T. Li, E. Wang and S. Dong, *Anal. Chem.*, 2010, **82**, 1515–1520.
40 D. Lu, L. He, Y. Wang, M. Xiong, M. Hu, H. Liang, S. Huan, X. B. Zhang and W. Tan, *Talanta*, 2017, **167**, 550.
41 W. Wang, Y. Jin, Y. Zhao, X. Yue and C. Zhang, *Biosens. Bioelectron.*, 2013, **41**, 137–142.
42 C. Liu and C. Z. Huang, *Chin. J. Anal. Chem.*, 2014, **42**, 1195–1198.
43 S. Zhan, Y. Wu, Y. Luo, L. Liu, L. He, H. Xing and P. Zhou, *Anal. Biochem.*, 2014, **462**, 19–25.
44 Z. Kahveci, R. Vazquez-Guillo, A. Mira, L. Martinez, A. Falco, R. Mallavia and C. R. Mateo, *Analyst*, 2016, **141**, 6287–6296.

 